Progress in Organic Coatings 88 (2015) 220–227

Contents lists available at ScienceDirect

Progress in Organic Coatings

journal homepage: www.elsevier.com/locate/porgcoat

Enhanced degree of polymerization of methacrylate and epoxy resins by plasmonic heating of embedded silver nanoparticles

Silvana V. Asmussen, Gustavo F. Arenas, Claudia I. Vallo*

Institute of Materials Science and Technology (INTEMA), University of Mar del Plata, CONICET, Juan B Justo 4302, 7600 Mar del Plata, Argentina

ARTICLE INFO

Article history:
Received 4 September 2014
Received in revised form 9 March 2015
Accepted 27 June 2015

Keywords:
Silver nanoparticles
Plasmonic heating
Post-curing
Photopolymerization

ABSTRACT

Silver nanoparticles (Ag NPs) were synthesized in situ in light-cured methacrylate and epoxy resins. The UV–vis spectra of the colloidal suspensions displayed an intense surface plasmon resonance band in the wavelength range 350–550 nm with an absorption peak at 415 nm. Suspensions containing different amounts of Ag NPs were photopolymerized by UV irradiation. Cylindrical specimens of the resulting nanocomposites (10-mm diameter × 1-mm thickness) were irradiated with a 420-nm LED source while the temperature evolution was monitored. The heat released by the Ag NPs under irradiation at the plasmon-resonant wavelength increases the temperature of the surrounding medium. The temperature reached in a methacrylate-based nanocomposite containing 0.03 wt% Ag NPs was 100 °C after 250 s irradiation. This increases the mobility of the reaction environment and, consequently, induces the polymerization of the unreacted monomer. Moreover, the degree of polymerization of films prepared from an epoxy resin containing 0.02 wt% Ag NPs was 35%, and then increased up to 75% after 10 min irradiation at 420 nm. In practice, the post-curing of partially cured polymers is commonly carried out by thermal treatments. Results obtained in this study show that the use of a small amount of Ag NPs, as controlled sources of heat under light irradiation, is an attractive strategy to post cure methacrylate and epoxy resins in the absence of external heating.

1. Introduction

Noble metal nanoparticles (NPs) can efficiently release heat under light irradiation [1–5]. The electromagnetic field strongly drives mobile carriers inside the NPs and the energy gained by these carriers is turned into heat. The heat then diffuses away from the NPs and leads to an elevated temperature of the surrounding medium. Heat generation in noble metal NPs induced by light absorption has long been considered only as a side effect, which had to be minimized. However, in the emerging field of thermoplasmonics the focus has shifted toward the design of optically induced nanoscale thermal sources. This opens up a new set of applications in nanotechnology and gives rise to the new promising field of plasmonic heating [4,5]. The number of potential applications of plasmonic heating is becoming increasingly important in areas of nanotechnology such as chemical catalysis [6], photo thermal cancer therapy [7], and materials processing [8–10]. Most of the research on plasmonic heating of noble NPs has been carried out on gold nanoparticles under laser irradiation. However, recent studies have shown that silver nanoparticles irradiated by light-emitting diodes (LEDs) are an interesting alternative [8,9]. Silver NPs have the advantages of possessing a stronger plasmonic heating effect [11], being cheaper than gold nanoparticles. In addition, the surface plasmon resonance of the Ag NPs can be controlled by changing the shape of the particles. Ag NPs with different shapes, such as spheres, pentagons, triangles, etc. can be easily synthesized [12], Spherical Ag NPs have a surface plasmon wavelength range between 400 and 450 nm, while the pentagon ones a 500–550 nm range and the triangular ones 650–700 nm [12]. As light with a longer wavelength generally has a lower price, longer wavelength LED lights should be considered from the economical point of view.

It is well known that the polymerization of methacrylate [13] and acrylate [14] monomers in the absence of external heating leads to glassy polymers in which only some of the available double bonds are reacted. As the polymerization proceeds, vitrification effects begin to limit the mobility of even small molecules such as the monomer or primary initiator radicals. Before completion of conversion, the vitrification phenomenon decelerates the reaction to a hardly perceptible rate. As shown by Kloosterboer and Lijten [15] the room temperature polymerization of the unreacted monomer proceed slowly for a long period. The presence of non-reacted monomer has a plasticizing effect on the polymer, thereby

* Corresponding author.
E-mail address: civallo@fi.mdp.edu.ar (C.I. Vallo).

http://dx.doi.org/10.1016/j.porgcoat.2015.06.032
0300-9440/

altering its physical and mechanical properties. In practice, the plasticizing effect of the non-reacted monomer on the mechanical behavior of the polymer is reduced by post-curing treatments. Heating the partially cured polymer increases the mobility of the reaction environment (i.e. monomer, radical and polymer) and consequently increases the degree of polymerization. The post-curing of incompletely cured polymers is commonly performed by thermal treatments. This study was carried out in order to explore the possibility of post-curing methacrylate and epoxy resins via plasmonic heating of embedded Ag NPs. This treatment has the advantages that require less equipment space and has lower energy consumption with respect to thermally-driven processes carried out in ovens. Thus, it can be considered more environmental friendly than other post-curing methods.

2. Experimental

2.1. Materials

Silver nitrate ($AgNO_3$ ≥99%, Aldrich) and absolute ethanol (Merck) were employed as received. The iodonium salt p-(octyloxyphenyl) phenyliodonium hexafluoroantimonate (Ph_2ISbF_6) (OMAN 071, 96%) was from Gelest Inc., Philadelphia, USA. Benzoyl peroxide (BPO, ≥97%), 1-phenyl-1,2-propanedione (PPD, 99%), 2,2-dimethoxy-2-phenylacetophenone (DMPA, 99%), ethyl-4-dimethylaminobenzoate (EDMAB, 99%) and 2,6-di-tert-butyl-p-cresol (BHT, ≥99%) were from Sigma Aldrich, USA.

The methacrylate resins used for this study were 2,2-bis[4-(2-hydroxy-3-methacryloxyprop-1-oxy)phenyl]-propane (BisGMA, 90%, from Esstech, Essington, PA), 2,2-bis[4-(2-methacryloxyethoxy)phenyl]propane (BisEMA, 98%, from Esstech, Essington, PA), and triethylene glycol dimethacrylate (TEGDMA, 95%, from Aldrich, USA). BisTEG stands for a blend 70:30 BisGMA/TEGDMA. The epoxy resin was 3,4-epoxycyclohexylmethyl 3′,4′-epoxycyclohexane carboxylate (UVR) (UVR-6110, 95%, Dow Chemical Co., Midland Michigan, USA). The resins were used without further purification. The methacrylate resins contain hydroquinone (HQ), hydroquinone methyl ether (MEHQ) and 2,6-di-tert-butyl-p-cresol (BHT) as inhibitors to prevent premature polymerization during storage. BisEMA contains 300 ppm MEQH and 200 ppm BHT. BisTEG contains 400 ppm MEQH, 5 ppm HQ, and 200 ppm BHT. Different amounts of each inhibitor are added to the methacrylate resins by the manufacturer in order to optimize the inhibition during storage and to minimize the increase in color produced by the inhibitors (yellowing). In all cases the Ag^+/reducer mol ratio equal to 1 was maintained by adding the required amount of BHT. Similarly, BHT at a mol fraction Ag^+/BHT equal to 1 was added to formulatios prepared from UVR. All materials were used as received. The structures of the resins and photoinitiators used are shown in Fig. 1.

The methacrylate resins were activated for UV light (365 nm) polymerization by the addition of 0.5 wt% DMPA. The epoxy resin containing 2 wt% iodonium salt (Ph_2ISbF_6) was activated for visible light (420 nm) polymerization by the addition of 1 wt% PPD and 1 wt% EDMAB. The light sources used were assembled from light emitting diodes (LED) with its irradiance centered at 365 nm (OTLH-0480-UV, Optotech) or 420 nm (LHUV-0420-0650, Luxeon-Phylips). The intensity of the 365-nm LED was 175 mW. The intensity of the 420-nm LED was set at two different values by varying the electrical voltage through the semiconductor: 200 and 1000 mW.

2.2. Preparation of suspensions of Ag NPs

Dispersions of colloidal silver particles were obtained by reduction of silver nitrate in methacrylate (BisEMA and BisTEG) and epoxy (UVR) resins in the absence of protective agents. $AgNO_3$ (0.126 g) was dissolved in 10 ml of absolute ethanol (solution A). The solution was stirred at room temperature until complete dissolution of the silver nitrate was achieved. Solution A was diluted with ethanol to volume ratio 1:5 (solution B) or 1:20 (solution C). Suspensions having different silver content were prepared by mixing 1 ml of the corresponding solution of $AgNO_3$ (A, B or C) with the appropriate amount of methacrylate or epoxy resin. The silver proportion in the resins was varied in the ranges: 3000–5000 ppm using solution A, 400–2000 ppm using solution B, and 50–300 ppm using solution C. In all cases, the required amount of ethanol was added in order to have a resin/ethanol mass ratio equal to 2. The reaction was carried out in glass tubes placed in a thermostat held at 70 °C allowing continuous evaporation of volatiles. The reaction was allowed to proceed for ~24 h in order to ensure complete evaporation of the ethanol. Silver cations were reduced by HQ, MEHQ and BHT present in the methacrylate resins.

2.3. Methods of characterization

The absorption spectra of dispersions of silver nanoparticles in methacrylate and epoxy resins were measured with an UV-vis spectrophotometer 1601 PC Shimadzu at room temperature (20 ± 2 °C). The dispersions were contained in thin cells (~0.5 mm) constructed from two quartz microscope slides separated by a PTFE gasket. An identical cell containing the resin was used as the reference.

The size distribution of silver NPs was determined using a Philips CM-12 transmission electron microscope (TEM) operated at an accelerating voltage of 100 kV. In order to obtain good quality images, the suspensions of silver nanoparticles in the resins were diluted with ethanol (1 drop of the resin in 600 μl de ethanol). Samples for TEM images were prepared by dropping 6 μl of the diluted dispersion of the particles on a copper grid coated with Formvar and a carbon film.

2.4. Photopolymerization studies

Fourier transform infrared (FTIR) spectra were acquired with a Nicolet 6700 Thermo Scientific. Measurements of C=C conversion in BisEMA and BisTEG methacrylate resins were carried out at room temperature (20 ± 2 °C) using near infrared spectroscopy (NIR). The NIR spectra were acquired over the range 4500–7000 cm^{-1} from 16 co-added scans at 2 cm^{-1} resolution. The resins were contained in a 10 mm diameter well constructed from a rubber gasket material sandwiched between two glass plates. The thickness of the samples was 2 mm. With the assembly positioned in a vertical position, the light source was placed in contact with the glass surface. The samples were irradiated at regular time intervals and the spectra were collected immediately after each exposure interval. These spectra were corrected with the background spectrum collected through an empty mold assembly fitted with only one glass slide to avoid internal reflectance patterns. The conversion profiles were calculated from the decay of the absorption band located at 6165 cm^{-1}. Two replicates were used in the measurement of conversion.

The conversion at the surface of 2 mm thick specimens of methacrylate resins was assessed by attenuated total reflectance using a diamond crystal. The conversion was evaluated from the decay of the band at 1637 cm^{-1} assigned to the methacrylate double bond. Spectra were obtained from 64 scans at 4 cm^{-1} resolution. Measurements of conversion of epoxy groups in UVR resin were carried out at room temperature (20 ± 2 °C) using mid-infrared spectroscopy (MIR). Spectra were acquired over the range 700–1200 cm^{-1} from 32 co-added scans at 2 cm^{-1} resolution. The resins were coated onto a polyethylene film and covered with another polyethylene film. The assembly was sandwiched between two NaCl plates and was tightly attached to the sample holder

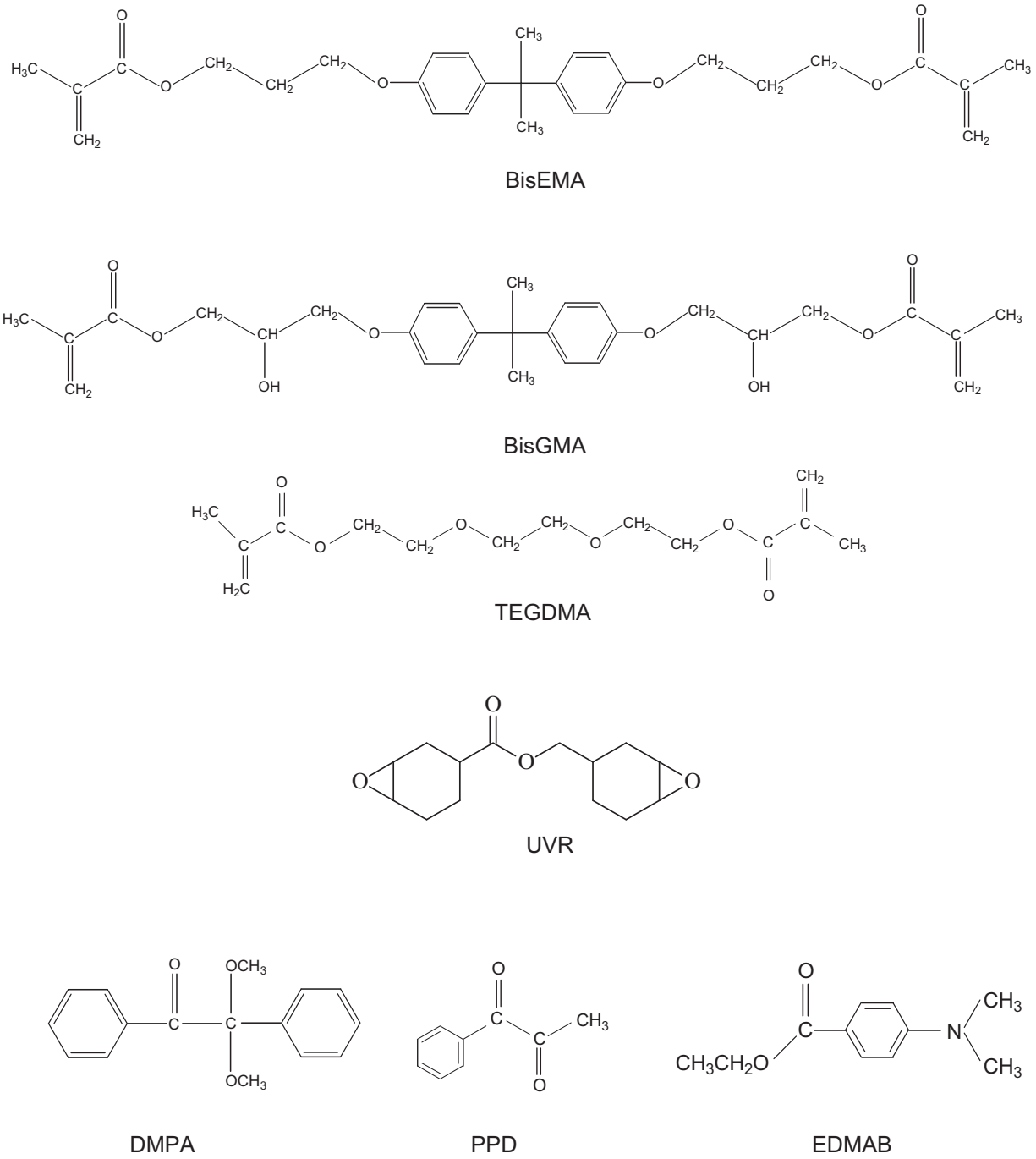

Fig. 1. Structure of the monomers and photoinitiators used in this study.

using small clamps. The thickness of the films was about 100 μm. The specimens were irradiated at regular time intervals and spectra were collected immediately after each exposure interval. The conversion of epoxy groups was calculated from the decay of the absorption band located at 788 cm^{-1} using as internal reference the peak centered at 1731 cm^{-1}.

2.5. Temperature evolution during irradiation of the resins

The resins were contained in a 10 mm diameter well constructed from a rubber gasket material sandwiched between two glass plates. The thickness of the specimens was 1 mm. The specimens were irradiated by placing the LED light source at 1 mm from the glass surface. The temperature of the samples during irradiation with the 420-nm LED was monitored with fine K-type thermocouples (Omega Engineering Inc., USA) embedded in the specimens and connected to a data acquisition system that registered values of temperature every 1 s. Two replicates were conducted for each experiment.

3. Results and discussion

3.1. Synthesis of Ag NPs in methacrylate and epoxy monomers

Ag NPs were in situ synthesized in methacrylate and epoxy monomers through reduction of $AgNO_3$ with HQ, MEHQ, and BHT,

in the absence of surfactant. Highly stable dispersions of Ag NPs in methacrylate and epoxy resins were synthesized using a straightforward one-step synthesis method. The suspensions showed a very intense yellow color, which became darker with increasing concentration of Ag NPs. A major obstacle preventing the formation of homogeneous Ag NPs/polymer suspensions arises from the poor compatibility of the two dissimilar constituents [16]. The use of organic capping agents is usually required in the synthesis of silver nanoparticles to control the agglomeration, particle size, and morphology. The capping agents carry specific functional groups to anchor them onto the surface of the nanoparticles, thereby preventing particle agglomeration and growth. It is well known that polymers are very effective to inhibit the agglomeration of nanosized particles. However, the effect of small molecules, such as monomers, on stability of colloidal metal particles is less known. The particle/polymer interaction and surface modification of particles in order to attain compatibility of the nanoparticles with the polymer matrix has been recently reviewed by Demir and Wegner [16]. The monomers investigated here, BisEMA, BisTEG and UVR have oxygen-containing groups capable of forming complexes with metal species [17]. Ag NPs interact with ester [18,19], ether [20,21], and hydroxyl groups [22] through no covalent bonding. Thus, it is conceivable that in a first stage Ag^+ ions disperse and coordinate to the oxygen atoms of those functional groups. Then, the reduction of the dispersed Ag^+ ions gives atomic silver which aggregate to form Ag NPs. Again, the oxygen-containing groups present in the monomer structures prevent precipitation and further aggregation of Ag NPs while stabilizes them. Thus, the ligand molecules bound to the nanoparticle surface not only control the growth of the particles during synthesis, but also prevent their aggregation during storage.

Stable suspensions of Ag NPs were obtained up to mass fractions equal to 0.02 wt% in UVR epoxy resin, and 0.03 and 0.5 wt% in BisEMA and BisTEG methacrylate resins, respectively. At silver mass fractions higher than these values precipitation occurred. The markedly higher stabilization ability of the BisTEG resin can be attributed to its particular molecular structure. The BisEMA and BisTEG monomers contain the same mol% of carbonyl and ether groups. However, in BisTEG the ratio phenyl alkyl ether (from BisGMA)/alkyl ether (from TEGDMA) is ~50/50 mol%. Although the mol of ether groups in BisEMA and BisTEG on weight basis is the same, we speculate that due to its greater flexibility, TEGDMA could probably arrange itself to provide better coverage on the surface of silver colloids compared with BisGMA and BisEMA. In addition, BisTEG contains hydroxyl groups in its structure. This could explain the better protection from agglomeration of BisTEG compared with BisEMA.

3.2. Characterization of the suspensions of Ag NPs

Fig. 2 shows the absorption spectra of BisEMA and UVR containing 0.02 and 0.03 wt% silver. The emission spectrum of the 420-nm LED is shown in the same plot. The Ag NPs exhibit a strong absorption maximum in the visible region (~415 nm) due to photon-induced oscillation of surface electrons (surface plasmon). After storage in air and in the dark for 9 months the silver sols were still clear, and the UV–vis spectra obtained after this storage period changed only a little. Since the reduction was performed in air it has to be expected that the silver nanoparticles are partially oxidized, due to the sensitivity of the colloidal silver nanoparticles toward oxidation [23]. Henglein has shown that such oxidation processes are associated with a strong decrease and broadening of the absorption bands [23]. The slight changes of the absorption bands after storage observed here, however, indicate that such oxidation processes either do not have a large influence with these protective monomers, or are completed after a short initial period.

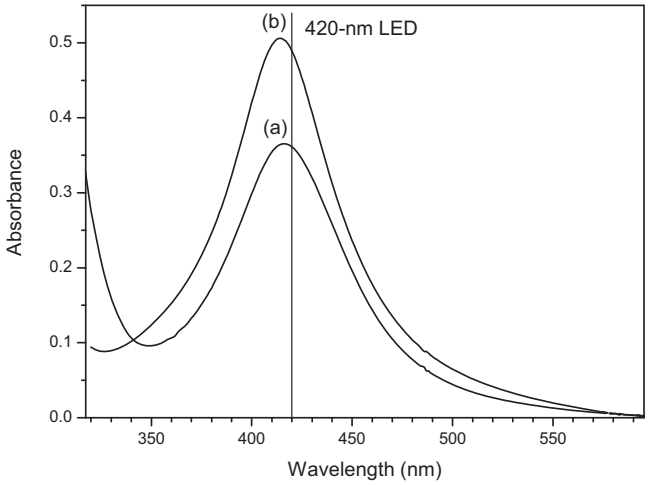

Fig. 2. UV–vis absorption spectra of (a) BisEMA and (b) UVR containing 0.02 and 0.03 wt% Ag NPs. The wavelength of the 420-nm LED is also shown.

Fig. 3 shows a typical photograph of Ag NPs dispersed in BisEMA. TEM images reveal that Ag NPs distribute homogeneously in the wide area of the photograph. The size of the particles in BisEMA, BisTEG and UVR monomers, calculated by measuring the diameters of at least 100 particles from the TEM images, was between 5 and 10 nm. UV–vis and TEM studies revealed that the suspensions stored for nine months, showed no drastic change in average particle size.

3.3. Photopolymerization of methacrylate monomers containing Ag NPs

BisEMA and BisTEG resins containing Ag NPs were photo activated with 0.5 wt% DMPA, which absorbs in the range 305–390 nm, and were photo polymerized with a LED of irradiance centered at 365 nm. Fig. 4 shows the conversion profiles of resins containing different amounts of Ag NPs. It is seen that as the Ag NPs concentration increased it became more difficult to cure the specimens. Although the final conversions in resins containing 0 or 300 ppm Ag NPs were similar, the polymerization rate decreased appreciably on increasing the Ag NPs concentration. It is worth mentioning that it has been reported that photoreduction of Ag^+ can occur in the presence of radicals derived from DMPA under irradiation at 365 nm [24]. However, the procedure used in this study to prepare

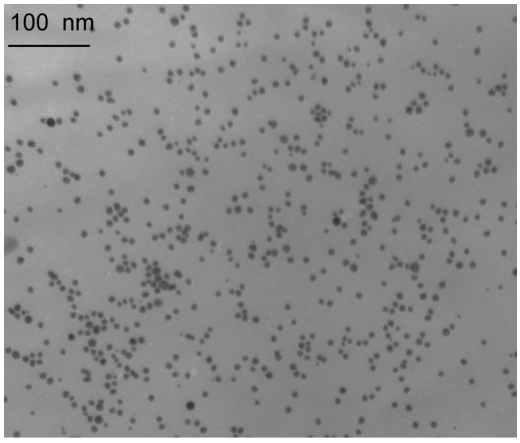

Fig. 3. Typical TEM image of a suspension of 300 ppm Ag NPs in BisEMA. The size of the particles in BisEMA, BisTEG and UVR monomers, calculated by measuring the diameters of at least 100 particles from the TEM images, was between 5 and 10 nm.

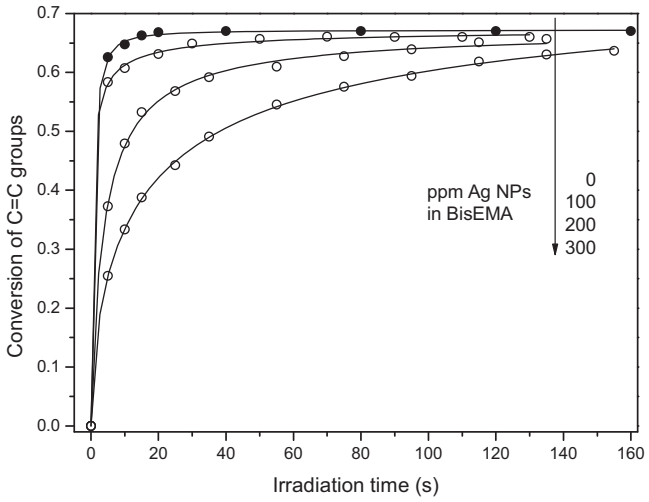

Fig. 4. Conversion of methacrylate groups measured by NIR vs. irradiation time in BisEMA monomer containing different amounts of Ag NPs (ppm). The resins were photo activated with 0.5 wt% DMPA and irradiated with a 365-nm LED.

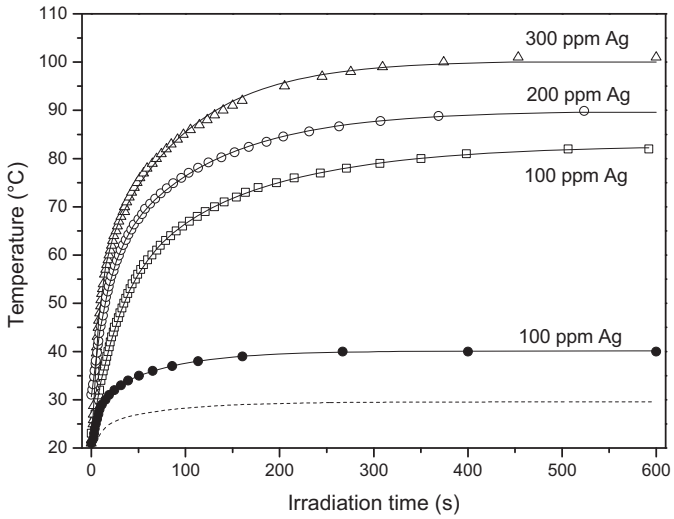

Fig. 5. Temperature evolution under irradiation of BisEMA containing different amounts of AgNPs with the 420-nm LED. Hollow symbols represent samples irradiated at 1000 mW. Filled circles represent a sample containing 100 ppm AgNPs irradiated at 200 mW. The specimens were 10-mm diameter and 1-mm thick. The dotted line is the temperature reached in BisEMA monomer in the absence of photoinitiator and Ag NPs.

Ag NPs/monomer colloids and the amount of reducer present in the formulations ensures that all the Ag^+ were reduced before photopolymerization.

When an assembly of nanoparticles is irradiated by a plane wave, the incident light is scattered and absorbed by each particle to a certain extent [25]. As a result of these absorption and scattering processes the transmitted light decreases along the propagation direction of the incident light [25]. The reduced polymerization rate with increasing Ag NPs content is attributed to the related decrease in light intensity along the irradiation path. It is worth mentioning that the polymerization of 1 mm thick specimen of BisTEG containing 0.1 wt% Ag NPs was incompletely cured even after 5 min de irradiation on both sides. Thus, the resins containing high proportions of Ag NPs (>0.1 wt%) were thermally cured with 1 wt% BPO at 80 °C for 1 h.

3.4. Enhanced conversion of methacrylate groups via plasmonic heating of Ag NPs

Noble metal NPs can efficiently release heat under light irradiation. The mechanism of generating heat is explained by converting electromagnetic energy into thermal energy. The electromagnetic field strongly drives mobile carriers inside the NPs and the energy gained by these carriers is turned into heat. The heat then diffuses away from the NPs and leads to an elevated temperature of the surrounding medium. Heat generation becomes especially strong in the regime of plasmon resonance, which is a collective motion of a large number of electrons [5]. Heat generation in noble metal nanoparticles (NPs) induced by light absorption has long been considered only as a side effect, which had to be minimized. Only recently this enhanced light absorption, turning metal NPs into nanosized sources of heat remotely controllable using light has been considered as a way to control thermal-induced phenomena at the nanoscale.

The plasmonic heating effect of Ag NPs on the degree of polymerization of methacrylate resins was investigated. In a first stage, suspensions containing different amounts of Ag NPs in methacrylate resins were photopolymerized by irradiation at 365 nm. In a second stage, cylindrical specimens of the resulting polymers (10-mm diameter × 1-mm thickness) were irradiated with the 420-nm LED while the temperature evolution was monitored. In order to achieve an optimal plasmonic heating effect, the wavelength of the LED source should approach the surface plasmon resonance wavelength of Ag NPs as closely as possible. The 420-nm LED used in the experiments is matched well with the plasmon wavelength of the Ag NPs in the methacrylate and epoxy resins (~415 nm), as shown in Fig. 2. The temperature evolution in BisEMA and BisTEG containing different amounts of Ag NPs upon irradiation with the 420-nm LED is shown in Figs. 5 and 6.

It is seen that the heat released by the Ag NPs under irradiation at the plasmon-resonant wavelength increases the temperature of the specimens. As expected, the temperature reached increases with light intensity (Fig. 5). At low Ag NPs content the temperature of the specimen increases with the Ag NPs content (Fig. 5). However, the temperature profiles in BisGMA containing 2500 and 5000 ppm Ag NPs were not markedly different (Fig. 6). This is attributed to the fact that the temperature profiles in the specimens are dictated by the competing mechanisms of light absorption and heat transference to the surroundings. In addition, as a result of the absorption and scattering of the incident light by the embedded particles, the transmitted light decreases along the irradiation path. This leads

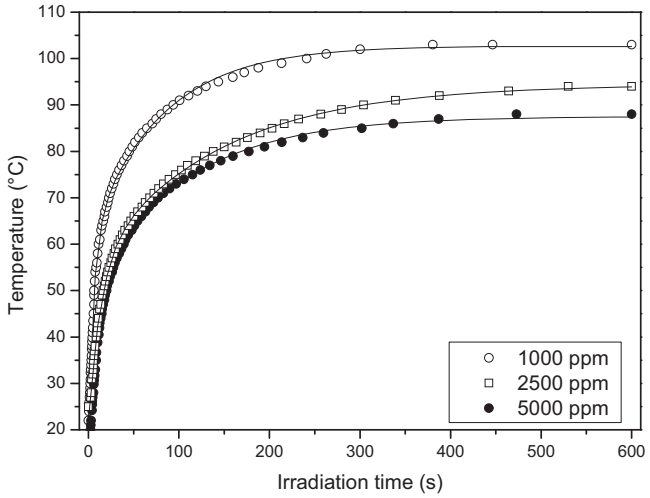

Fig. 6. Temperature evolution under irradiation of BisTEG containing different amounts of AgNPs with the 420-nm LED. All the samples were irradiated at 1000 mW.

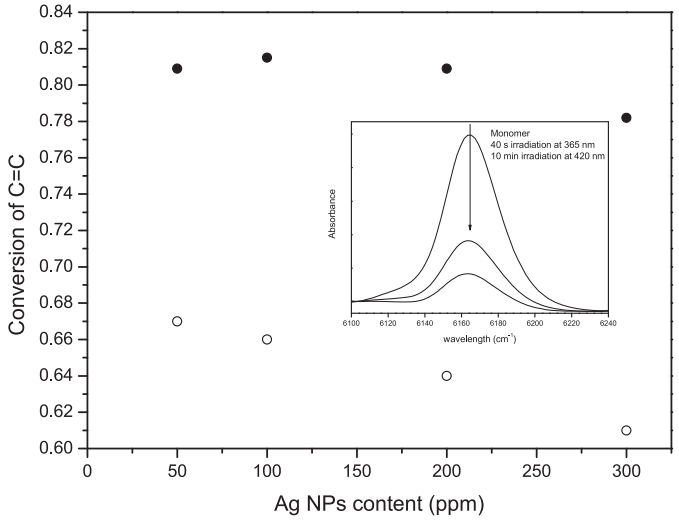

Fig. 7. Extent of reaction reached in samples containing 0.5 wt% DMPA irradiated 120 s with the 365-nm LED (hollow circles), and samples irradiated 10 min with the 420-nm LED after the first irradiation at 365 nm (filled circles). The specimens were 10-mm diameter and 1-mm thick. Typical NIR bands of the monomer, a sample irradiated 40 s at 365 nm and a sample irradiated 10 min at 420 nm.

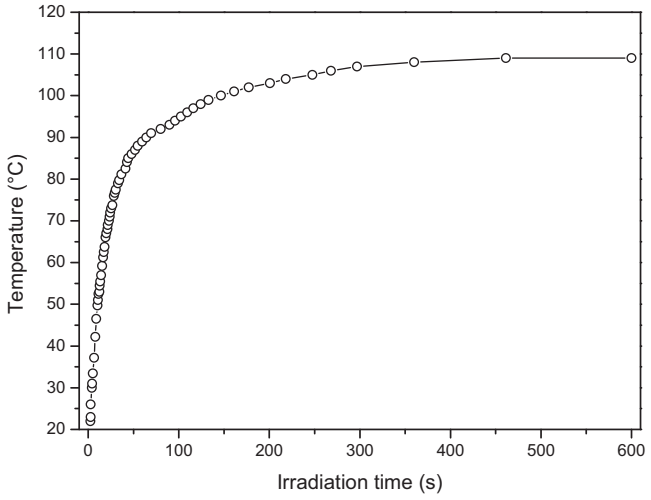

Fig. 8. Temperature evolution during irradiation of BisEMA containing 300 ppm AgNPs and 1 wt% BPO with the 420-nm LED. The heat released by the AgNPs under irradiation results in the thermal decomposition of BPO, which initiates the polymerization reaction. The conversion of methacrylate groups measured by ATR after 10 min irradiation was 0.83. The specimens were 10-mm diameter and 1-mm thick.

to a reduced absorption of light over the thickness of the specimen and, in turn, to a lower plasmonic heating of the Ag NPs. From these results it may be concluded that, under the experimental conditions used in this study, the maximum temperature increase occurs at a content of Ag NPs equal to 300 ppm.

The presence of unreacted monomer (Fig. 4, BisEMA without Ag NPs) has a plasticizing effect on the polymer, thereby altering the physical and mechanical properties of the hardened material [26]. In practice, the plasticizing effect of the unreacted monomer on the mechanical behavior of the polymer is reduced by a post-curing treatment. Heating the partially cured polymer at a temperature above its glass transition temperature increases the mobility of the reaction environment (i.e. monomer, radical and polymer) and consequently increases the reaction rate parameters. This thermal treatment increases the degree of polymerization and, consequently, reduces the plasticizing effect of the unreacted monomer [26]. In practice, there are many processing routes to produce parts and components that involve post-curing treatments. For example, coatings of automotive exterior body panels for trucks and cars processed by sheet molded compound are subjected to heat treatments of post-curing [27]. Parts prepared by sheet molded compound from urethane diacrylate resins are post cured in convection ovens at 90 °C for 30 min after UV-curing [28]. Organic–inorganic hybrid coatings based on acrylate resins and silanes are UV cured at room temperature and then annealed at either 80 °C [29] or 100 °C [30] for 24 h in order to achieve high degree of cross-linking. The room temperature polymerization of 2-hydroxyethyl methacrylate, which is widely used in biomedical applications, is followed by a post curing for 2 h at 100 °C to complete the polymerization [31]. Epoxy resins are also subjected to post cure treatments. The room temperature polymerization of an epoxy resin based on diglycidyl ether of bisphenol A and triethylenetetramine is followed by a post curing treatment at 80 °C for 4 h [32].

In this study, the post-curing of methacrylate resins via plasmonic heating of Ag NPs embedded in the incompletely cured polymers was examined. BisEMA resins containing 0.5 wt% DMPA and different contents of Ag NPs were irradiated for 120 s with the 365-nm LED. In a second stage, the partially cured polymers were irradiated with the 420-nm LED during 10 min. Fig. 7 shows that the irradiation at 420 nm increases appreciably the extent of polymerization of methacrylate groups. The Ag NPs act as sources of heat remotely controllable by light, thereby providing an alternative way to perform post-curing treatments. It must be pointed out that the degree of polymerization increases with the intensity of the LED source and with irradiation time. We limited the irradiation to 10 min in order to protect the LED source, which was designed for research purposes. However, the use of commercially available high intensity LEDs will result in increased degree of polymerization during the post-curing treatment. The post-curing treatment via plasmonic heating of embedded Ag NPs has the advantages that require less equipment space and has lower energy consumption with respect to themal-driven processes carried out in ovens. Thus, it can be considered more environmental friendly than other post-curing methods. In addition, the plasmonic heating effect is observed at low Ag NPs contents (~300 ppm). From these results it is concluded that plasmonic heating is an attractive strategy to perform the post-curing of methacrylate monomers in the absence of external heating. Ag NPs are incorporated to different monomers in many application of technological interest [33]. Some of the applications include optical filters [34], dental restorative resins [35] and coatings with antibacterial activity [36,37]. The presence of Ag NPs in these applications would permit the post curing treatment, when required, via irradiation with light at the proper wavelength.

The use of plasmonic heating of noble metal nanoparticles to perform the photo induced polymerization of methacrylate monomers, in the absence of light-absorbing photoinitiators, was examined. The BisEMA resin containing 300 ppm Ag NPs and 1 wt% BPO was irradiated with the 420-nm LED. Fig. 8 shows the temperature profile during irradiation of the specimen. The heat released by the Ag NPs under irradiation with light at the plasmon resonance wavelength of Ag NPs results in the thermal decomposition of BPO, which initiates the polymerization. The conversion of methacrylate groups after 10 min irradiation in the absence of external heating was 0.83 (Table 1). It is worth noting that the room temperature polymerization of BisEMA containing BPO under irradiation with a 420-nm LED in the absence of Ag NPs does not occur. From these results, it may be concluded that the use of Ag NPs, as controlled sources of heat under light irradiation, enables the photo induced polymerization of methacrylate groups in the absence of photoinitiator and external heating.

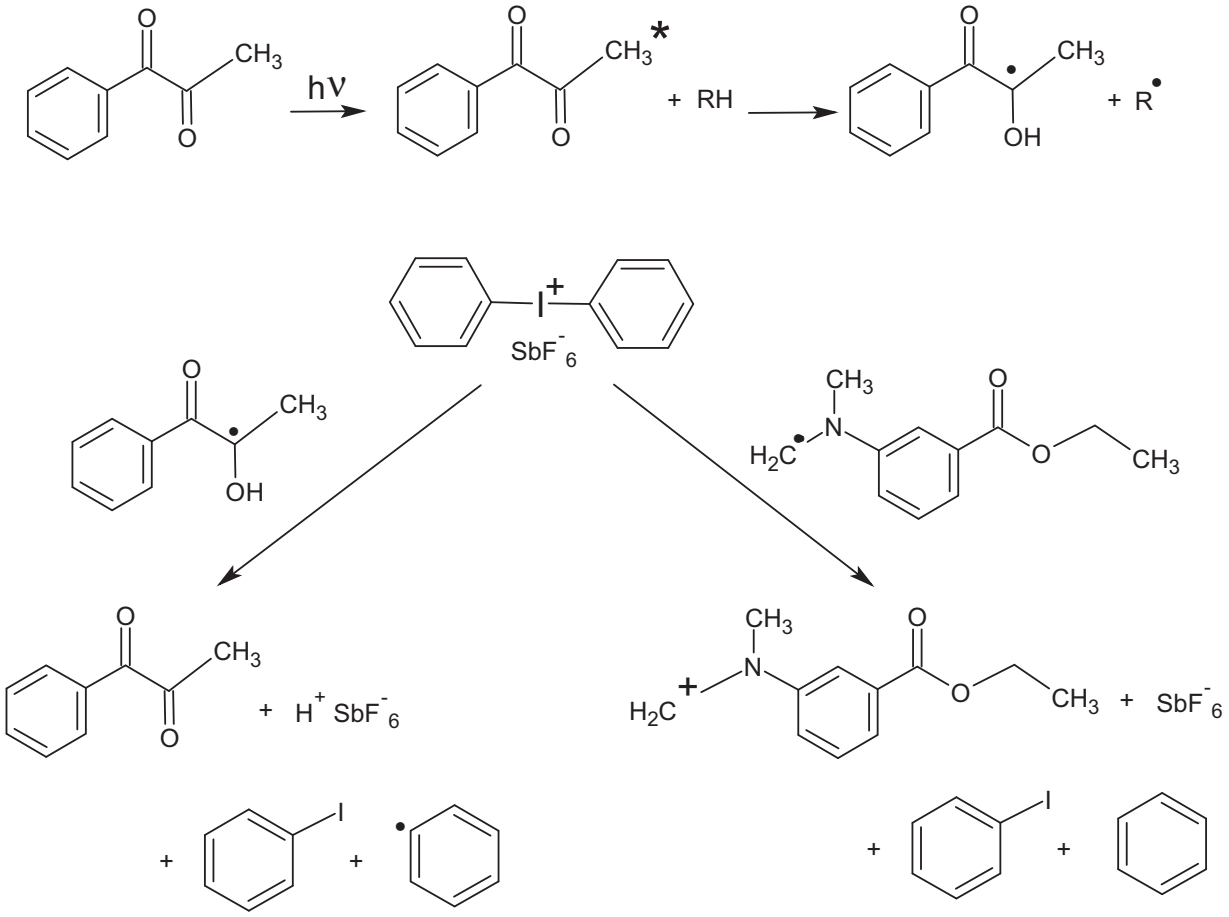

Fig. 9. Proposed photosensitization of Ph_2ISbF_6 by PPD the presence of EDMAB.

3.5. Polymerization of epoxy monomers enhanced by plasmonic heating

Cationic photopolymerization has become an important method of crosslinking epoxy monomers, and onium salts are well known as very effective photoinitiators. The use of cationic photoinitiators, such as diaryliodonium and triarylsulfonium salts, provides a convenient method of generating powerful Brønsted acids in situ, which is the primary species that initiates polymerization. By using dyes as photo sensitizers, it is possible to extend the spectral sensitivity of diaryliodonium salts into the visible region of the spectrum. For example, Camphorquinone (CQ), which absorbs at 470 nm, in combination with electron donating co-initiators such as ethyl-4-dimethyl aminobenzoate (EDMAB), acts as an efficient visible light photo sensitizer in the iodonium-initiated cationic polymerization of epoxy monomers [38]. Concerning the reactivity of the UVR epoxy monomer, Crivello and Varlemann [39] found that it undergoes photopolymerization at slow rate and reaches a comparatively low extent of reaction. In a previous research, we reported the polymerization of the UVR monomer photoactivated with Ph_2ISbF_6/CQ/EDMAB. We found that the polymerization rate of the UVR was strongly affected by the cure temperature [38]. From results obtained in this study (Figs. 5–7), it was conceived that the heating of the UVR resin containing Ag NPs under irradiation with a 420-nm LED could induce further conversion of epoxy groups. In order to test that hypothesis, the effect of plasmonic heating of Ag NPs on the extent of reaction of UVR was examined. The UVR resin was activated for visible light polymerization by the addition of 2 wt% Ph_2ISbF_6, 1 wt% PPD and 1 wt% EDMAB. Fig. 9 shows the proposed photosensitization of Ph_2ISbF_6 by PPD the presence of EDMAB. PPD in combination with EDMAB (Fig. 1) produces initiating free radicals through a bimolecular mechanism [40]. PPD is activated from below 350 nm to 490 nm with a maximum at about 390 nm [40]. Thus, the 420-nm LED is appropriate to generate initiating radicals from the PPD/EDMAB pair as well as to induce the plasmonic heating of the Ag NPs embedded in the resin. Irradiation of the PPD with 420-nm light results in the formation of its singlet state, which is rapidly converted to its triplet state by intersystem crossing. The excited PPD molecule is initially reduced by a hydrogen donor (in our case the amine) to the ketyl radical which in turn is oxidized back to CQ by the iodonium salt. The resulting strong Brønsted acid derived from this process initiates the cationic ring-opening polymerization. In the case of the CQ/EDMAB pair, the mechanism is analogous to that proposed by Bi and Neckers [41] for the visible light cationic polymerization of cyclohexene oxide in the presence of a diaryliodonium salt.

Table 1
Increased conversion of epoxy and methacrylate groups in BisEMA and UVR resins containing embedded Ag NPs. The resins were irradiated for 600 s with a 420-nm LED. The conversion of BisEMA was measured by ATR. Note that the room temperature polymerization of BisEMA containing BPO under irradiation with a 420-nm LED in the absence of Ag NPs does not occur.

Resin	Photoinitiator	Ag NPs (ppm)	Conversion
BisEMA	BPO	0	–
BisEMA	BPO	300	0.83
UVR	Ph_2ISbF_6/PPD/EDMAB	0	0.31
UVR	Ph_2ISbF_6/PPD/EDMAB	200	0.75

Table 1 shows the conversion reached in films of UVR photoactivated with Ph_2ISbF_6/PPD/EDMAB and irradiated with the 420-nm LED. Results presented in Table 1 reveal that, in analogy with CQ/EDMAB, the PPD/EDMAB pair efficiently photo initiates the polymerization of UVR monomer under irradiation at 420 nm. It is seen that the extent of reaction of the epoxy monomer was markedly increased by the presence of Ag NPs. The conversion reached in the absence of Ag NPs was 0.31 and increased to 0.75 in the same resin containing 200 ppm Ag NPs. This is attributed to the heating of the Ag NPs embedded in the films under irradiation with the 420-nm LED. Again, the heating of the films induces an increase in the mobility of the reaction environment and consequently increases the degree of polymerization. Results presented in Table 1 show that the presence of 200 ppm Ag NPs is an effective way to increase the extent of reaction of the UVR epoxy monomer.

4. Conclusion

The plasmonic heating effect of Ag NPs embedded in methacrylate resins was assessed by measuring the temperature evolution of specimens during irradiation with a 420-nm LED. The temperature reached in a 10-mm diameter x 1-mm thickness specimen containing 300 ppm Ag NPs was 100 °C after 250 s irradiation. The heating produced under irradiation of methacrylate and epoxy resins containing embedded Ag NPs results in a marked increase in the extent of polymerization. The principle of plasmonic heating of Ag NPs under 420-nm light irradiation can be used to perform the polymerization of a dimethacrylate monomer initiated by benzoyl peroxide in the absence of photoinitiator. The heat released by the Ag NPs on irradiation at 420 nm results in the thermal decomposition of the benzoyl peroxide, which initiates the polymerization. From result obtained in this research, it may be concluded that the use of Ag NPs, as controlled sources of heat under light irradiation, increase the degree of polymerization of methacrylate and epoxy monomers in the absence of external heating, and enables the photo induced polymerization of methacrylate groups in the absence of light absorbing photoinitiators.

Acknowledgements

The financial support provided by the ANPCyT and CONICET is gratefully acknowledged. The authors are grateful to Esstech for the generous donation of the methacrylate monomers used in this study.

References

[1] A. Govorov, W. Zhang, T. Skeini, H. Richardson, J. Lee, N. Kotov, Nano. Res. Lett. 1 (2006) 84.
[2] A. Govorov, H. Richardson, Nanotoday 2 (2010) 30.
[3] G. Baffou, R. Quidant, C. Girard, Appl. Phys. Lett. 94 (2009) 153109.
[4] T. Baffou, R. Quidant, Laser Photonics Rev. 7 (2013) 171.
[5] S. Boriskina, H. Ghasemi, G. Chen, Mater. Today 16 (2013) 375.
[6] J. Adleman, D. Boyd, D. Goodwin, D. Psaltis, Nano Lett. 9 (2009) 4417.
[7] X. Huang, M. El-Sayed, Alex. J. Med. 47 (2011) 1.
[8] Y. Li, T. Verbiest, R. Strobbeb, I. Vankelecom, J. Mater. Chem. A 1 (2013) 15031.
[9] Y. Li, T. Verbiest, R. Strobbeb, I. Vankelecom, J. Mater. Chem. A 2 (2014) 3182.
[10] S. Maity, L. Downen, J. Bochinski, L. Clarke, Polymer 52 (2011) 1674.
[11] A.O. Govorov, H.H. Richardson, Nano Today 2 (2007) 30.
[12] B. Wiley, Y. Sun, B. Mayers, Y. Xia, Chem. Eur. J. 11 (2005) 454.
[13] N. Alemdar, B. Karagoz, A.T. Erciyes, N. Bicak, Prog. Org. Coat. 60 (2007) 69.
[14] F. Bauer, U. Decker, S. Naumov, C. Riedelc, Prog. Org. Coat. 77 (2014) 1085.
[15] J.G. Kloosterboer, G.F. Lijten, Polymer 31 (1990) 95.
[16] M. Demir, G. Wegner, Macromol. Mater. Eng. 297 (2012) 838.
[17] A. Pomogailo, D. Wöhrle, in: F. Ciardelli, E. Tsuchida, D. Wöhrle (Eds.), Macromolecule–Metal Complexes, Springer, Berlin, 1996, p. 53.
[18] R. Sardar, J. Park, J. Shumaker-Parry, Langmuir 23 (2007) 11883.
[19] N. Nikonorova, E. Barmatov, D. Pebalk, M. Barmatova, G. Dominguez-Espinosa, R. Diaz-Calleja, et al., J. Phys. Chem. C 111 (2007) 8451.
[20] L. Longenberger, G. Mills, J. Phys. Chem. 99 (1995) 475.
[21] T. Sakai, P. Alexandridis, Chem. Mater. 18 (2006) 2577.
[22] A. Tolstov, V. Matyushov, E. Lebedev, D. Klimchuk, Theor. Exp. Chem. 47 (2012) 371.
[23] A. Henglein, Chem. Mater. 10 (1998) 444.
[24] R. Nazar, S. Ronchetti, I. Roppolo, M. Sangermano, R.M. Bongiovanni, Macromol. Mater. Eng. 300 (2015) 226.
[25] M. Quinten, Optical Properties of Nanoparticle Systems, Wiley-VCH Verlag & Co. KGaA, Germany, 2011.
[26] C. Vallo, J. Biomed. Mater. Res. Appl. Biomater. 53 (2000) 717.
[27] M.G. Smolka, A. Müller, U. Gohs, A. Calvimontes, Prog. Org. Coat. 72 (2011) 159.
[28] S.M. Trey, M. Lundström, D. Ståhlberg, M. Johansson, Plast. Rubber Compos. 38 (2009) 131.
[29] F. Khelifa, M. Druart, Y. Habibi, F. Bénard, P. Leclère, M. Olivier, P. Dubois, Prog. Org. Coat. 76 (2013) 900.
[30] Y. Mülazim, E. Cakmakc, M.V. Kahraman, Prog. Org. Coat. 72 (2011) 394.
[31] L.V. Karabanova, G. Boiteux, G. Seytre, I. Stevenson, O. Gain, C. Hakme, E.D. Lutsyk, A. Svyatyna, J. Non Cryst. Solids 355 (2009) 1453.
[32] T.K. Bindu Sharmila, A.B. Nair, B.T. Abraham, P. Sabura Beegum, E. Thachil, Polymer 55 (2014) 3614.
[33] D. Pozo Perez (Ed.), Silver Nanoparticles, In Tech, 2010, ISBN: 978-953-307-028-5 http://www.intechopen.com/books
[34] G. Carotenuto, M. Palomba, A. Longo, S. De Nicola, L. Nicolais, Sci. Eng. Compos. Mater. 18 (2011) 187.
[35] C. Fan, L. Chu, H.R. Rawls, B.K. Norling, H.L. Cardenas, K. Whang, Dent. Mater. 27 (2011) 322.
[36] R.D. Toker, N.K. Apohan, M.V. Kahraman, Prog. Org. Coat. 76 (2013) 1243.
[37] M. Akbarian, M.E. Olya, M. Ataeefard, M. Mahdavian, Prog. Org. Coat. 75 (2012) 344.
[38] W. Schroeder, S. Asmussen, M. Sangermano, C. Vallo, Polym. Int. 62 (2013) 1368.
[39] J. Crivello, U. Varlemann, J. Polym. Sci. Polym. Chem. 33 (1995) 2473.
[40] W. Schroeder, G. Arenas, C. Vallo, Polym. Int. 56 (2007) 1099.
[41] Y. Bi, D. Neckers, Macromolecules 27 (1994) 3683.